The Journal of Experimental Biology 209, 1904-1913
Published by The Company of Biologists 2006
doi:10.1242/jeb.02223

Partial coherence and other optical delicacies of lepidopteran superposition eyes

D. G. Stavenga
Department of Neurobiophysics, University of Groningen, NL 9747 AG Groningen, The Netherlands
e-mail: D.G.Stavenga@rug.nl

Accepted 20 March 2006

Summary

Superposition eyes are generally thought to function ideally when the eye is spherical and with rhabdom tips in the focal plane of the imaging optics of facet lenses and crystalline cones. Anatomical data as well as direct optical measurements demonstrate that the superposition eyes of moths and skippers often deviate severely from the expected ideal case. Part of the deviation has been attributed to diffraction at the single facet lens, which was taken to be an essential limit to spatial resolution, because light traveling through different facet lenses was assumed to be incoherent. By considering the two-dimensional facet lens lattice, it is here demonstrated that many facets within a superposition aperture transmit coherent light, allowing a much sharper image than possible with single facet lens diffraction. Partial coherence therefore is an important aspect of superposition imaging. It is argued that broadening of the photoreceptor acceptance angles occurs because of optical errors in the facet lens-crystalline cone system other than diffraction. The transmittance of the superposition aperture of moths and skippers is improved by the corneal nipple arrays of the facet lenses, but quantitative assessment shows that the effect is minor.

Key words: diffraction, corneal nipple array, moth, Lepidoptera, skipper, optical path length.

Introduction

Lepidoptera, the insect order consisting of the butterflies and moths, use two different types of compound eyes, namely apposition and superposition eyes (Exner, 1891; Exner, 1989; Kunze, 1979; Land, 1981). Both eye types are composed of ommatidia, where a facet lens and crystalline cone form the imaging optics, and the light-sensitive rhabdomeres of the photoreceptor cells are joined into a fused rhabdom. In apposition eyes, a single facet lens focuses light from a distant point source onto the light-sensitive rhabdom, whereas in superposition eyes several facets jointly relay the incident light to a rhabdom. The light sensitivity of the superposition eye is therefore superior to that of the apposition eye, and accordingly the two eye types are associated with different life styles: the diurnally active papilionoid butterflies have apposition eyes and the nocturnal moths have superposition eyes. All superposition eyes encountered among the Lepidoptera are of the refractive superposition eye type, where refractive index gradients in the crystalline cone cause the redirection of incident light. In the reflective superposition eyes of many crustaceans this redirection occurs as a result of reflective layers facing the cones (Land and Nilsson, 2002).

The spatial resolution of butterfly apposition eyes appears to be superior to that of the superposition eyes of most moths, which is attributed to focusing errors intrinsic to the superposition eye design. However, many diurnal moths and also the diurnally active and visually acute skipper butterflies (Hesperoidea) rely on superposition eyes. The structural details and the optical properties of the diurnal superposition eyes subtly differ from those of the nocturnal eyes, suggesting that they reflect adaptations that circumvent the shortcomings of superposition optics (Warrant and McIntyre, 1993; Warrant et al., 2003).

For a superposition eye to work well, it is presumed to combine a spherical eye shape with well-focusing crystalline cones in equal-sized ommatidia in all eye parts, resulting in the same spatial acuity throughout the eye (Exner, 1891; Land, 1981; Nilsson, 1989; Warrant et al., 2003). Whereas most superposition eyes seem to satisfy this rule, the diurnal hawkmoth *Macroglossum stellatarum* radically departs from it (Warrant et al., 1999). The hawkmoth eye is quite aspherical; it has extensive gradients in resolution and sensitivity, and a frontal acute zone provides the eye with extremely sharp and bright images. The anatomy is most aberrant in that the eye locally has more rhabdoms than facets, frontal-ventrally by a factor of more than four (Warrant et al., 1999). These findings necessitate a closer look into the optics of lepidopteran superposition eyes.

In the present study, the optical requirements for ideal superposition optics are revisited and compared with the optics of real eyes, leading to the conclusion that severe deviations of ideal superposition exist. The accepted view is that light beams through different facets interact incoherently, so that spatial resolution of superposition eyes is limited by single lens

Table 1. *Anatomical data for the moths and skippers studied*

	Moths		Skippers						
Anatomical data (μm)	*E.ku.*	*P.tr.*	*T.sy.*	*T.pe.*	*N.re.*	*T.pa.*	*H.pi.*	*O.wa.*	*H.or.*
Facet lens diameter, D_l	20	24	30	21	25	20	20	22	20
Eye radius, R	340	694	1080	690	800	600	750	650	760
Length of cornea and cone, c	55	94	110	100	110	100	95	90	90
Width of clear zone, w	85	117	440	290	370	240	150	130	280
Rhabdom layer curvature, r	200	483	530	300	330	260	505	430	390

Moths: *E.ku.*, Ephestia kühniella (Cleary et al., 1977; Kunze, 1979); *P.tr.*, *Phalaenoides tristifica* (Horridge et al., 1977; Land, 1984)
Skippers: *T.sy.*, *Trapezitis symmomus*; *T.pe.*, *Toxidia peroni*; *N.re.*, *Netrocoryne repanda*; *T.pa.*, *Taractrocera papyria*; *H.pi.*, *Hesperilla picta*; *O.wa.*, *Ocybadistes walkeri*; *H.or.*, *Hesperilla ornata* (Horridge et al., 1972; Land, 1984); see also Fig. 2.

diffraction (Land, 1984; Warrant et al., 1999). However, it will be shown that multiple sets of facets contribute coherent light to a superposition image and that coherence plays a substantial role in superposition eye imaging. In addition, the possible optical function of the corneal nipples at the facet lenses of lepidopterans is investigated. Their contribution to vision is concluded to be minor. A survey of the optical components that determine spatial resolution and light sensitivity shows that superposition eyes can have excellent spatial resolution, no worse than that of butterflies, as has been demonstrated experimentally (Horridge et al., 1977; Land, 1984; Warrant et al., 1999), but optical errors in the imaging by the facet lens–crystalline cone combination can substantially degrade superposition eye vision.

Materials and methods

Anatomical data of moth and skipper eyes

The quantitative evaluations are based on the anatomical data of moth and skipper eyes of Table 1, derived from various sources (Cleary et al., 1977; Horridge et al., 1972; Horridge et al., 1977; Kunze, 1979; Land, 1984).

Theory of angular magnification and aperture of an ideal superposition eye

In an ideal superposition eye, light from a point source at infinity enters through a large set of facet lenses, and these lenses, together with the underlying crystalline cones, focus the incident light onto the tip of a single rhabdom (Fig. 1). Following Land (Land, 1984), we first restrict ourselves to the light rays through the vertices of the facet lenses. Fig. 2A shows such a light ray with angle of incidence at the eye surface α, which is thus a multiple of the interommatidial angle. The ray leaves the crystalline cone with an exit angle β, which is the angle between the light ray and the ommatidial axis. In an ideal superposition eye all rays that enter through the facet lens vertices proceed as oblique rays through the clear zone, which then converge on the tip of the rhabdom located at point P. The angular magnification, $m=\beta/\alpha$, must therefore change with the angle of incidence according to Eqn 1 (assuming α is small and in radians):

$$m(\alpha) = (1/\alpha) \arctan[2r\alpha / (r\alpha^2+2w)] , \quad (1)$$

where r is the radius of curvature of the distal surface of the rhabdom layer, and w is the width of the clear zone between crystalline cones and rhabdom layer (Fig. 2). Their sum, $r+w=p$, is the radius of curvature of the proximal cone tips, and with the joint length of the facet lens and crystalline cone, c, the radius of curvature of the eye surface is $R=p+c$ (Fig. 2A).

The aperture of a superposition eye is determined by the maximal angle of incidence, α_{max}, of rays that reach the clear zone below the crystalline cone. The associated exit angle is β_{max}. Rays through facet lenses with $\alpha>\alpha_{max}$ thus no longer contribute to the superposition image, because they are absorbed by the screening pigment layers that surround the crystalline cones (Fig. 1). Whereas α_{max} strongly depends on the species, β_{max} appears to be remarkably constant among a diverse range of animals with refractive superposition eyes: $\beta_{max}\approx30°$ in the moth *Ephestia kühniella* (Cleary et al., 1977),

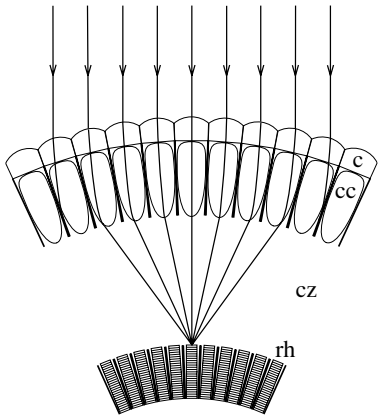

Fig. 1. Diagram of an ideal refracting superposition eye in the dark-adapted state. Light entering an eye first passes the corneal facet lenses (c) and subsequently the crystalline cones (cc). Proximal to the array of crystalline cones is the clear zone (cz) and the layer of rhabdoms (rh). A beam of light parallel to the optical axis of an ommatidium is focused on the rhabdom of the central ommatidium. Sheets of screening pigment surround the crystalline cones. In many species, tracheolar tapeta and/or screening pigment isolate the rhabdoms from each other. The set of facets that contributes to the superposition image of a distant point source is called the superposition aperture.

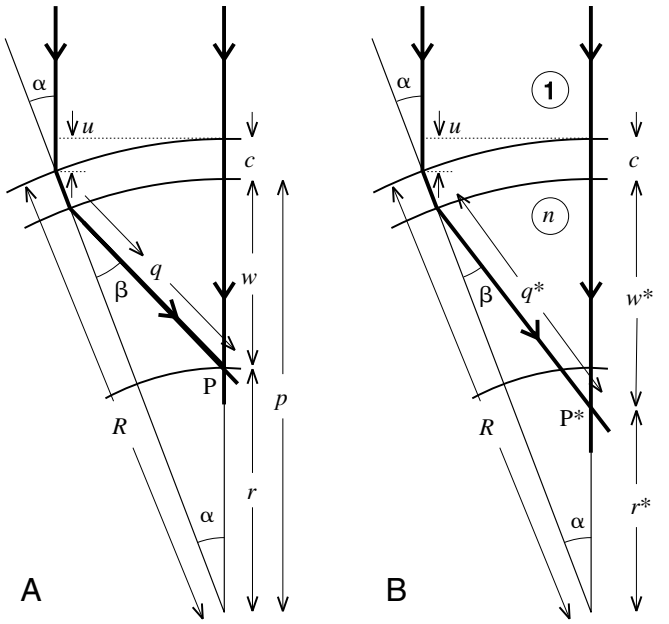

Fig. 2. Schematic light paths in a superposition eye (modified from Land, 1984). (A) Focal point at the retinal surface. r is the radius of curvature of the distal surface of the rhabdom layer, w is the clear zone width, i.e. the distance of the rhabdom layer surface to the proximal tips of the crystalline cones, and c is the thickness of the crystalline cone and facet lens layer. $R=r+w+c$ is the radius of the corneal outer surface, or the eye radius, and $p=r+w$ is the radius of curvature of the proximal cone tips. α is the angle of incidence of a ray through the vertex of a facet, and the angle of that ray with the ommatidial axis after having passed the facet lens and crystalline cone is the exit angle β. The central ray is defined by $\alpha=\beta=0$. The oblique ray travels a distance q in the clear zone before intersecting the central ray at point P, which ideally coincides with the tip of the central rhabdom. (B) Focal point proximal to the retinal surface. The focal point P* is then located at a distance r^* from the center of curvature of the eye and w^* from the proximal cone tip. The distance traveled across the clear zone by the oblique ray is q^*. The difference in optical path lengths of the two rays in point P* is $u+nq^*-nw^*=u+n(q^*-w^*)$, where u is the path length difference between the ray with incident angle, α, and the central ray, when reaching the corneal surface, and n is the refractive index of the eye tissue.

dung beetles *Onitis aygulus*, *O. alexis* and *O. westermanni* (McIntyre and Caveney, 1985) and euphausiid *Meganyctiphanes norvegica* (Land et al., 1979), as well as in reflective superposition eyes of crayfish (Bryceson and McIntyre, 1983). The angular magnification $m(\beta)$ has therefore been calculated for $0<\beta<30°$ using Eqn 1 and $\beta=m\alpha$.

Angle-dependent defocus with a constant angular magnification

The light rays of a parallel beam emitted by a distant point source converge after having passed the facet lenses and crystalline cones (Fig. 2). The central ray, with angle of incidence $\alpha=0$, proceeds in the same direction ($\beta=0$). When the angular magnification, m, is constant, it follows that the rays through the facet lens vertices do not converge to one and the same point. Generally, a ray with angle of incidence α intersects the central ray at a point P*, with distance r^* to the center of curvature of the eye (Fig. 2B):

$$r^* = p\sin\beta / \sin(\alpha+\beta) . \quad (2)$$

The rays through different facet lenses have different intersection or focal points, located at a defocus distance $\delta=r-r^*$ from the rhabdom tip. This distance is a function of the angle of incidence, α, or equivalently, of the exit angle, β.

Optical path length difference

The optical path length (OPL) difference of the two rays of Fig. 2 at the point of intersection P* is:

$$\Delta\mathrm{OPL} = u^* + n(q^* - w^*) , \quad (3)$$

where $u^*=2R[\sin(\alpha/2)]^2$, $q^*=p\sin\alpha/\sin(\alpha+\beta)$ and $w^*=p[1-\sin\beta/\sin(\alpha+\beta)]$ (see Land, 1984).

Coherence length

The criterion for interference of two light rays emitted by a point source and arriving at an image point *via* different pathways is that the difference in optical path length, ΔOPL, must be smaller than the (longitudinal) coherence length l_c (Mandel and Wolf, 1995, p.149f), which is given by:

$$l_c = \bar{\lambda}^2 / \Delta\lambda , \quad (4)$$

where $\bar{\lambda}$ is the average wavelength and Δλ the bandwidth of the light. For visual systems, the coherence length is determined by the spectral sensitivity of the photoreceptors. The main photoreceptors of most eyes, and certainly of moth eyes, are green receptors with peak wavelengths 530 nm, for example *P. tristifica* (Horridge et al., 1977), and half-width 100 nm, and hence the coherence length may be taken as 2.8 μm.

Fraunhofer diffraction for a circular aperture and an annulus

When a parallel beam of monochromatic light with wavelength λ passes a (facet) lens, with diameter D_l, radius $a_l=D_l/2$, and focal distance f_l, the light distribution in the focal plane is given by the Airy expression (Born and Wolf, 1975):

$$I(s) = \{[\pi a_l^2 / (\lambda f_l)]\, B(v)\}^2 , \quad (5a)$$

where $B(v)=2J_1(v)/v$ with $v=[2\pi a_l/(\lambda f_l)]s$, and s is the distance from the axis, assuming a light beam with unit flux density, 1 W μm^{-2} [J_1 is the first order Bessel function (see also Stavenga, 2003)]. The corresponding formula for the diffraction pattern resulting from an annulus with outer and inner radius a_o and a_i is:

$$I(s) = \{[\pi a_o^2 / (\lambda f_l)]\, B(v_o) - [\pi a_i^2 / (\lambda f_l)]\, B(v_i)\}^2 , \quad (5b)$$

where $v_{o,i}=[2\pi a_{o,i}/(\lambda f_l)]s$.

Reflectance of the corneal nipple array

The outer surface of the facet lenses in moth and skipper eyes consists of an array of cuticular protuberances termed corneal nipples (Bernhard and Miller, 1962). Their optical

action is a reduction of the reflectance of the facet lens surface. The reflectance reduction can be quantitatively assessed from the nipple shape and dimensions. The nipples are assumed to be arranged in a hexagonal (or more correctly a triagonal) lattice, with distance between the nipples d=220 nm and nipple peak height h=250 nm. Two types of nipple shape are considered, with a parabolic and sinusoidal cross-section. The effective refractive index is calculated as a function of the distance from the facet lens substrate, with refractive index 1.52 (Vogt, 1974), using effective medium theory. The reflectance of the corneal nipple layer then can be calculated with standard multilayer formula (for details, see Stavenga et al., 2006).

Results

Angular magnification and defocus

We first consider the concept of an ideal superposition eye, which states that all light rays emerging from a distant point source converge to one and the same focal point, located at the tip of a rhabdom (Fig. 1). This means that for perfect focusing the angular magnification, m=β/α, should depend on the angle of incidence, α: $m(\alpha)=(1/\alpha)\arctan[2r\alpha/(r\alpha^2+2w)]$ (Eqn 1), where r is the distance of the rhabdom tip from the eye center, and w the width of the clear zone (Fig. 2). Using published anatomical data (Table 1), the angular magnification required for an ideal superposition eye has been calculated for a number of moths and skippers. Fig. 3 gives the results as a function of the exit angle β instead of α, because the literature data show that β has a more or less fixed range of 0–30° in all species with superposition eyes.

The calculated angular magnification values appear to be rather independent of the exit angle for all species, but the values for the different species widely vary. The results can be compared with published experimental data for the nocturnal moth *Ephestia kühniella* and the skipper *Toxidia peroni*. For *E. kühniella*, Fig. 3 predicts m=2.3–2.0, but ray tracing calculations based on refractive index measurements yielded a constant m=1.32 (Cleary et al., 1977). For *T. peroni*, Fig. 3 predicts m=1.0–0.6, but direct measurements yielded a fairly constant m=1.6. Ray tracing, on the other hand, suggested m=1.1 (Horridge et al., 1972). The agreement between the angular magnification values for an ideal superposition eye and the literature data is clearly not impressive, which questions the reliability of conclusions for the optical properties based on anatomy. The assumption that the focal plane of the superposition eye coincides with the distal surface of the rhabdom layer seems to be especially doubtful (e.g. Land, 1984).

Fig. 3 predicts the highest angular magnification of 4.1–3.6 for the diurnal moth *Phalaeonoides tristifica*, but those values are probably too large. The extreme angle of incidence was estimated to be α_{max}=11.4° (Land, 1984), and from $\beta_{max}\approx$30° it follows that $m\approx$2.6. An angular magnification lower than the ideal value means that the incident light rays do not converge at the rhabdom tips but instead at a more proximal level. Fig. 4 shows the defocus distance, $\delta=r-p\sin\beta/\sin[\beta(1/m+1)]$ (see Materials and methods, Eqn 2), for the two moth species, using the angular magnification value 1.32 for *E. kühniella* and 2.6 for *P. tristifica*. It appears that in both cases the focus is located at a distinctly deeper level than expected for an ideal superposition eye. A less severe situation will exist for most of the skippers, which are expected to have an angular magnification of about 1. When indeed $m\approx$1, the defocus will be quite minor. Nevertheless, in general the concept of well-focused superposition eyes must be applied with great caution (McIntyre and Caveney, 1998).

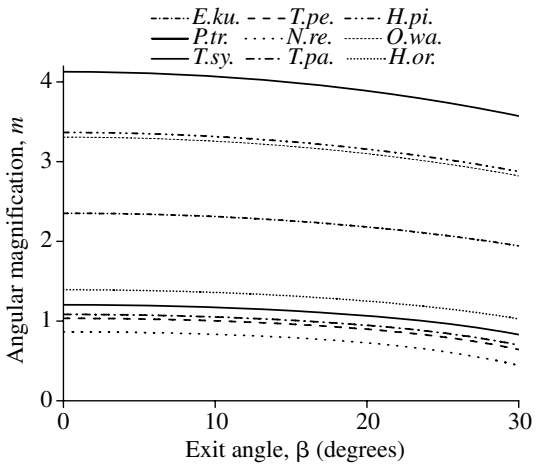

Fig. 3. Angular magnification, m, as a function of the exit angle, β, calculated for the moths and skippers listed in Table 1 with the condition that the superposition eyes are ideal, that is, all incident light rays from a distant point source are assumed to converge at the tip of one and the same rhabdom (see Fig. 1). For species abbreviations, see Table 1.

Optical path length difference

Next we investigate the view that the light beams passing through different facets in a superposition eye do not interfere because of lack of coherence (Land, 1984), and therefore we

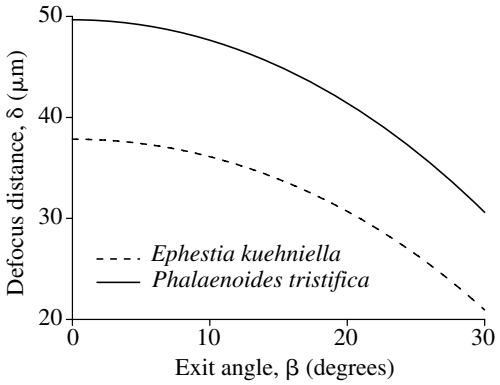

Fig. 4. Defocus distance for two moth species as a function of the exit angle, with angular magnification m=1.32 for *E. kühniella* and m=2.6 for *P. tristifica*.

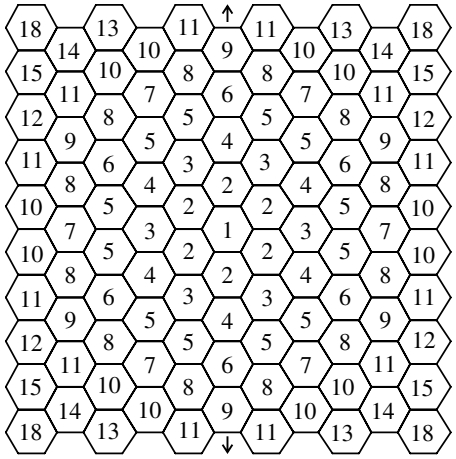

Fig. 5. Facet lens lattice with numbers, where the facets are classified according to their distance from the central facet, number 1. The facets 1, 2, 4, 6, 9, etc. are the facets of adjacent ommatidia in a meridional section (indicated by arrows). Rays parallel to the central ray (the ray through the vertex of facet 1) that travel through equal-numbered facets have the same optical path length difference with the central ray.

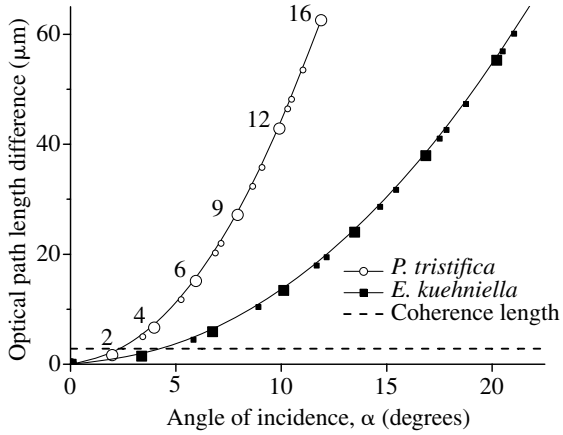

Fig. 6. Optical path length difference and coherence length of the diurnal moth *P. tristifica* and the nocturnal moth *E. kühniella*. The numbers adjacent to the large symbols indicate facets in a meridional row (Fig. 5). The optical path length difference between rays passing through the facets marked by the number 2 and a central ray passing through facet 1, is smaller than the coherence length of light for the green-sensitive photoreceptors (l_c=2.8 μm). This also holds between rays passing through facet pairs 7 and 8, 13 and 14, and 16 and 17.

return to the two rays of Fig. 2A, meeting each other at a point P. Their optical path length difference, $\Delta OPL = 2R[\sin(\alpha/2)]^2 + np\{[\sin\alpha + \sin(m\alpha)]/\sin[\alpha(1+m)] - 1\}$ (see Materials and methods), depends on the angle of incidence, or, equivalently, on the distance of the facets in the corneal lattice. To estimate the optical path lengths of rays traveling through different facets, we consider the facets in the hexagonal lattice of Fig. 5. The facets are numbered according to their distance from the central facet (number 1). The rays emerging from a distant point source that pass through facets with equal numbers will converge at the same intersection point P, and will thus have the same optical path length difference with the central ray.

Fig. 6 shows the optical path length difference as a function of the angle of incidence for the nocturnal moth *E. kühniella* and the diurnal moth *P. tristifica*, calculated with Eqn 3 and using the dimensions of Table 1. The two curves are presented as a function of the angle of incidence, α. Because the maximum angle of incidence α_{max} for *E. kühniella* is 22.5° (Cleary et al., 1977) and for *P. tristifica* α_{max}=11.4° (Land, 1984), the curves virtually coincide when plotted as a function of the exit angle, β. The difference in optical path length, ΔOPL, of rays through facets 2 with respect to those through facet 1 appears to be distinctly smaller than the coherence length l_c=2.8 μm for green receptors (see Materials and methods), but the ΔOPLs for the other adjacent facets in a meridional section (4, 6, 9, etc.) well exceed the coherence length. Yet, there are several cases where the optical path length differences of rays going through facets with subsequent numbers are smaller than the coherence length, for example for rays passing through facet pairs 7 and 8, 13 and 14, and 16 and 17 (Fig. 6). We thus have to conclude that partial coherence can play an important role in superposition eye imaging.

Coherence and diffraction patterns

To explore the possible effect of coherently cooperating facets on image sharpness, we consider a monochromatic light beam incident parallel to the axis of the ommatidium of facet 1 (Fig. 5). In the two-dimensional ommatidial lattice, the facets with the same numeral k transmit light rays with equal ΔOPL. The set of facets with the same tag number k surround the central facet in an annulus with radius r_k, the distance of the center of facet k to the center of facet 1. For k=2, 3, 4, 5, 6… the ratio of r_k and the facet lens diameter, D_l, is r_k/D_l=1, $\sqrt{3}$, 2, $\sqrt{7}$, 3, …., and the number of facets in the annuli with the same numeral is N_k=6, 6, 6, 12, 6, …. We can therefore consider the contribution to the image of the light waves passing through equally tagged facets as to result from an annulus with area $N_k(\pi D_l^2/4)$. When the width of the annulus, w_k, is small, the area of the annulus equals $2\pi r_k w_k$, yielding $w_k = N_k D_l^2/(8r_k)$. Diffraction patterns can then be calculated for each annulus, using Eqn 5b, with the outer radius $a_o = r_k + w_k/2$ and inner radius $a_i = r_k - w_k/2$.

The Fraunhofer diffraction patterns obtained for the diurnal moth *P. tristifica* for a 530 nm light beam are shown in Fig. 7. The curves in Fig. 7A present the light distribution patterns as a function of the distance, s, from the beam axis in the focal plane, resulting from imaging by the central facet (k=1) as well as by a few surrounding annuli (k=2–6), assuming a focal distance of f_l=200 μm. Notice that the peak height is proportional to the square of the number of cooperating facets in an annulus. This occurs because light intensity (or irradiance) is proportional to the square of the amplitude of the electromagnetic wave (see Materials and methods, Eqn 5). Fig. 7B presents the same data normalized and as a function of the angle $\theta = s/f_l$. The full halfwidth of the single facet

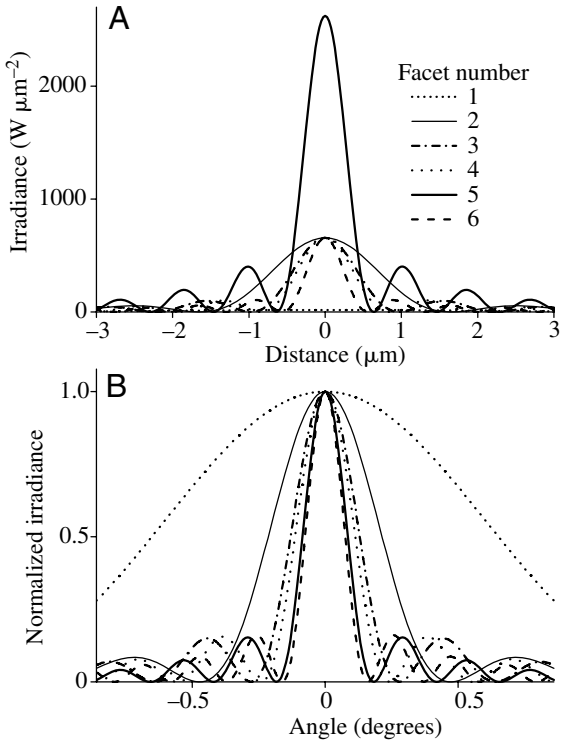

Fig. 7. Fraunhofer diffraction patterns of facet annuli for the diurnal moth *P. tristifica*, where the facet lens diameter is 24 μm, for monochromatic light with wavelength 530 nm. The light flux density at the corneal level is 1 W μm^{-2}. (A) The light distribution in the focal plane of the facet lens–crystalline cone system, assuming a focal distance of 200 μm. The irradiance due to the single, central facet is low and spread out. The peak irradiance resulting from the sets of 6 facets with numbers 2, 3, 4 and 6 is 36 times higher than that of the central facet, and the peak irradiance due to light from the set of 12 facets with number 5 is 144 times higher. (B) Normalized light patterns plotted as a function of the angle. The angle is the lateral distance of a divided by the focal distance. The width of the light distribution patterns reduces with increasing radius of the annuli.

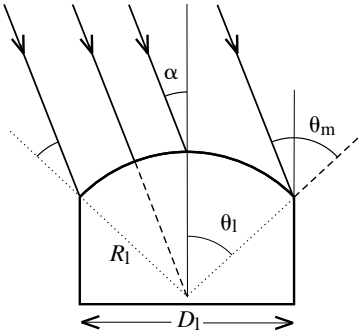

Fig. 8. Diagram of a facet lens with obliquely incident light. A light ray parallel to the ray through the lens vertex, arriving at the facet lens margin has an angle of incidence $\theta_m=\alpha+\theta_l$, where $\theta_l=\arctan(D_l/2R_l)$, with D_l the facet lens diameter and R_l the radius of the facet lens front surface.

diffraction pattern is 1.30° (the approximative formula $\Delta\rho_l=\lambda/D_l$ yields $\Delta\rho_l=1.27°$ with $\lambda=0.53$ μm and $D_l=24$ μm; Table 1). Fig. 7B shows that the width of the diffraction pattern narrows with increasing annulus diameter. The higher order annuli clearly produce extremely narrow diffraction patterns, far superior to that of a single facet lens.

The corneal nipple array of moth eyes

The irradiances of Fig. 7 have been calculated with the implicit assumption that the transmittance of the optics, that is the facet lens–crystalline cone combination, is the same for all facets and equal to 1. This is certainly not correct, as the transmittance gradually decreases towards the edge of the aperture (Cleary et al., 1977). It can be envisaged that the transmittance decrease results from the progressive tilt of the facets, which firstly causes a decreasing aperture (Navarro and Franceschini, 1998), and secondly an increasing reflectance. The latter effect might be effectively suppressed by an intriguing optical structure present in the facet lenses of moths (Bernhard et al., 1965; Horridge et al., 1977; Miller, 1979) and skippers (Horridge et al., 1972), namely the corneal nipple array, which is formed by nanosized protuberances at the facet lens surface. It is well known that the nipple array decreases the eye reflectance and thus enhances the facet lens transmittance (Miller, 1979), but because the reflectance is only a few percent at small angles of incidence, the transmittance enhancement, and thus the visual function of the corneal nipples, seems to be negligible. Yet, facet lenses with convex front surfaces form the surface of most superposition eyes, and light enters the facet lenses progressively more obliquely with increasing angles of incidence (Fig. 8). The rapid increase of the reflectance of a smooth surface at very oblique angles of incidence might severely compromise the efficiency of superposition imaging.

To investigate this, we consider a ray of a parallel beam entering at the lens margin, which has an angle of incidence $\theta_m=\alpha+\theta_l$, where θ_l is the aperture angle of the facet lens surface (Fig. 8). For the moth *E. kühniella*, the value of α for facet lenses at the rim of the superposition aperture is $\alpha_{max}\approx22.5°$ (Cleary et al., 1977). Because $\theta_l=\arctan(D_l/2R_l)$, it follows for $D_l=20$ μm and $R_l=14$ μm (Table 1) that $\theta_l\approx35.5°$ (Kunze, 1979). The incident angle at the facet lens margin thus may reach the quite considerable value of $\theta_m\approx58°$, an oblique angle at which reflectance may be substantial.

The reflectance of a moth eye with a nipple array can be readily understood by considering the nipple dimensions. Fig. 9 shows two nipple shapes, with parabolic and sinusoid cross-sections, with the same height $h=250$ nm, corresponding to the height found experimentally for moth and skipper eyes (Bernhard et al., 1965; Horridge et al., 1972; Horridge et al., 1977). The nipples are hexagonally packed in large, regular domains, where the nipples are spaced at a distance of about $d=220$ nm. The nipple distance is distinctly smaller than the wavelength of light, and the nipple layer therefore acts on incident light as a continuous interface with an effective

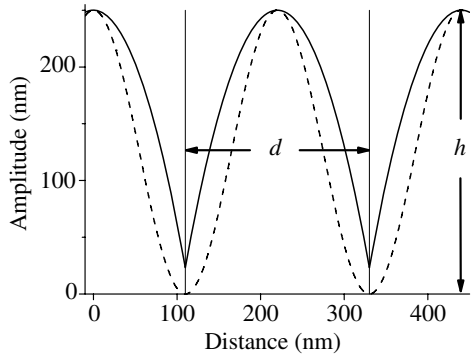

Fig. 9. Diagram of two types of corneal nipples, with parabolic and sinusoidal cross-section. The corneal nipples are spaced at a distance of d=220 nm, and they have a height h=250 nm. The paraboloid is chosen so that the area at its base equals the area of the unit lattice cell, and has at the base a radius $r_0=d\sqrt{\sqrt{3}/2\pi}$=116 nm. The radius of the sinusoid at the base is $r_0=d/2$=110 nm.

refractive index that gradually increases from 1.0 (air) to 1.52, the refractive index of the corneal material (Vogt, 1974). The effective refractive index of the nipple layer, calculated from the volume fraction of the corneal material using effective medium theory (Stavenga et al., 2006), is very approximately a linear function of the distance from the lens surface for the paraboloid nipples, but for the sinusoidally shaped nipples it has a more hyperbolic shape (Fig. 10).

The effect of the gradual change in refractive index on the reflectance can be straightforwardly calculated with a multilayer model (Stavenga et al., 2006). Fig. 11 presents the reflectance as a function of the angle of incidence for the two types of linear polarized light, TE and TM (electric vectors perpendicular and parallel to the plane of incidence, respectively), with wavelength 530 nm. It appears that the nipple array strongly reduces the reflectance at angles of incidence up to about 50°, especially for TE waves, but the reflectance rapidly rises at very oblique angles, above 60°. This behavior occurs for all wavelengths in the visible range.

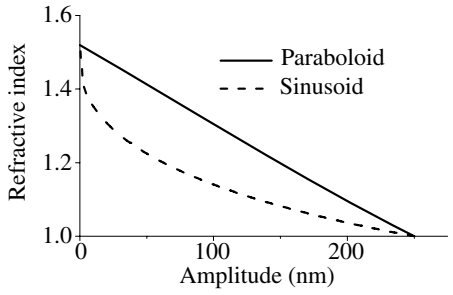

Fig. 10. The effective refractive index for paraboloid and sinusoidally shaped nipples calculated for a corneal nipple layer. For the paraboloid nipples, the effective refractive index decreases virtually linearly from the facet lens substrate (amplitude 0 nm) to the nipple tips (amplitude 250 nm), but for the sinusoidal nipples the decrease is more abrupt.

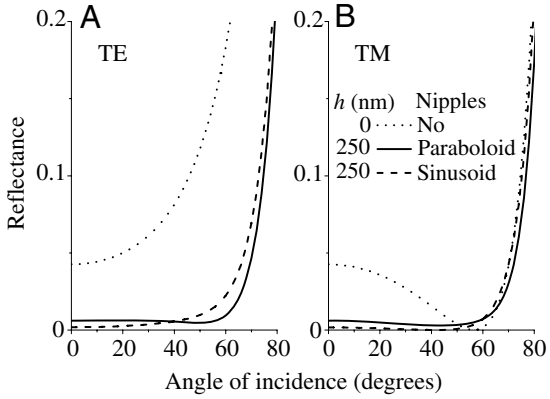

Fig. 11. The reflectance of the facet lens surface with paraboloid and sinusoidal nipples as a function of the angle of incidence and polarization, for light of wavelength 530 nm. The value of the refractive index of the facet lens medium is 1.52 (Vogt, 1974). (A) The reflectance for TE waves. (B) The reflectance for TM waves. For a smooth surface, that is in the absence of nipples, the reflectance for TM waves falls to zero at the Brewster's angle $\alpha=\arctan(1.52)=56.7°$. Both types of nipples strongly reduce the reflectance at angles of incidence below 50°, but at larger values the reflectance rapidly rises. A Brewster's angle only exists in the absence of nipples.

Whereas the reflectance reduction hardly depends on the exact shape of the nipples, their height appears to be a critical factor (Stavenga et al., 2006).

The calculations show that the nipple array of moth eyes is very effective in reducing the reflectance over a large range of angles of incidence. However, the effect on eye transmittance must be considered to be minimal. Fig. 11 shows that the enhancement of the transmittance is only a few percent, even in the extreme case of a marginal light ray with an angle of incidence of 58°. Actually, ray tracing studies show that these marginal rays do not contribute to the superposition image, as they are blocked by the crystalline cones (Cleary et al., 1977; McIntyre and Caveney, 1985). We therefore have to conclude that the corneal nipple array has no great beneficial consequences for vision, and therefore probably its main function is glare reduction to avoid detection by predatory birds (see also Miller, 1979; Stavenga et al., 2006).

Discussion

Partial coherence of light and the superposition image

A parallel beam of incident light enters a superposition eye through several facet lenses and crystalline cones and then travels through the clear zone before reaching the rhabdom layer. Because the superposition image is due to the cooperation of numerous facets, the full superposition aperture might be supposed to determine the diffraction limit. Snyder, however (Snyder, 1979, p. 251), stated that the image quality of a superposition eye is limited by the diffraction of the individual facet, but he provided no further proof or argument.

Diffraction is a wave-optical phenomenon where light waves interfere. In usual treatments of light diffraction by apertures it is implicitly assumed that all the light entering the aperture is coherent. Land was the first (and so far only one) to discuss a crucial limitation of wave-optical imaging in superposition eyes, namely the lack of coherence of the light beams traveling through different facets (Land, 1984). The criterion for interference of two light rays emitted by a source and arriving at an image point *via* different pathways is that the difference in optical path length must be smaller than the coherence length. Land concluded, in his pioneering study on the moth *P. tristifica* and the skipper *O. walkeri* (Land, 1984), that light traveling through a certain facet is incoherent with light that travels through the other facets. However, he calculated only the path length differences of rays through facets in a meridional section, whereas rays through all facets in the two-dimensional corneal lattice should have been considered (Fig. 5). It then appears that there are numerous sets of 6 or 12 facets that transmit coherent light. Fig. 6 furthermore reveals that the optical path length differences of several of these sets of facets are smaller than the coherence length 2.8 μm. Although Land's treatment implicitly assumed an ideal, perfectly focused superposition eye, so that the derived values for the optical path length differences are slightly too large, the conclusion that the resolution of superposition eyes is limited by diffraction at single facet lenses is too conservative, certainly with a coherence length value of 5 μm assumed (Land, 1984). It means that the coherence of light passing through different facets must be taken into account in superposition imaging.

The aperture transmittance

Another important factor that influences superposition imaging is the transmittance of the superposition aperture. This decreases with increasing distance from the axis, which is caused by a number of factors. Firstly, the reflectance at the front surface of the facet lenses, although small, reduces the transmittance. As demonstrated in Fig. 11, the corneal nipples in the facet lens front surface of moths and skippers effectively diminish the surface reflectance over a large range of angles of incidence, α. Although rather small in absolute terms, the resulting enhancement in transmittance will not be disadvantageous. A second cause for a reduction in transmittance is the progressive tilt of the facets towards the periphery of the aperture (Navarro and Franceschini, 1998). This obliquity factor is maximally $\cos(\alpha_{max})$, or, in the moths *E. kühniella* and *P. tristifica* with α_{max}=11.4° and 22.5°, it is at most 0.98 and 0.92, which means a transmittance reduction of maximally 2% or 8%.

The main component limiting the transmittance is the crystalline cone. The refractive index gradients in the cone can only cause convergence and redirection of an incident light beam for a small range of angles of incidence α and, consequently, exit angles β. With increasing angle of incidence α, the fraction of light rays that proceeds into the clear zone decreases, meaning a decreasing transmittance (Cleary et al., 1977; McIntyre and Caveney, 1985). The transmittance can be described by $T(\beta)=T_0(1-\beta/\beta_{max})^3$, with $\beta_{max}\approx30°$ and $T_0\leqslant1$, depending on the species (D.G.S., manuscript in preparation).

Fraunhofer diffraction

The calculated diffraction patterns of Fig. 7 are due to annuli of facets with the same number, that is, facets transmitting rays with identical optical path lengths to their focal point. The cooperative effect of neighboring facets with optical path length differences smaller than the coherence length will result in even narrower diffraction patterns than those of Fig. 7. We have to note, however, that only the facets with number 2 form a closed ring. The facets with higher numerals form interrupted annuli, and therefore the resulting diffraction patterns will lack circular symmetry and be less sharp than those calculated. Nevertheless, we can safely conclude that coherent imaging by several facets produces much sharper diffraction patterns than that due to a single facet. That, in principle, enables superior visual acuity.

Photoreceptor acceptance angle

Light that has passed the clear zone and reached the rhabdom layer can be absorbed there by the visual pigments in the rhabdoms. The half-width of the normalized amount of light absorbed as a function of the angle of incidence is the acceptance angle of the photoreceptors, $\Delta\rho$. The acceptance angle is determined by the geometrical width of the rhabdoms, diffraction of the imaging optics and errors in the focusing. It is customary to assume that the geometrical acceptance angle of the rhabdom is $\Delta\rho_r=D_r/r$, where D_r is the distal rhabdom diameter and r is the local radius of curvature of the layer of rhabdom tips (Land, 1984) (see Fig. 2). However, the effective geometrical acceptance angle of the rhabdom is $\Delta\rho_r=D_p/r$, where D_p is the diameter of the ommatidial aperture at the rhabdom tip level, at least when each rhabdom is surrounded by a tracheolar tapetum and/or sheath of pigment, as is the case in most moths and skippers (Land and Nilsson, 2002). For the diurnal moth *P. tristifica*, the diameter of the stop created by dark pigment is D_p=12 μm, and r=483 μm (Land, 1984), so that $\Delta\rho_r$=1.42°. In the skipper *O. walkeri*, the tracheolar tapetum has a diameter D_p=9 μm distally, which together with r=430 μm (Horridge et al., 1972) (Table 1) yields $\Delta\rho_r$=1.20°. In the latter case Land estimated r=323 μm, and then $\Delta\rho_r$=1.60° (Land, 1984). Using the light reflection on the tapetum, Land could visualize the retinal surface ophthalmoscopically, and he thus measured the acceptance angle $\Delta\rho$ as 1.58° and 2.18° for the moth and skipper, respectively (Land, 1984). The geometrical acceptance angles are hence smaller than the measured acceptance angles.

Land interpreted these differences (Land, 1984) as solely due to diffraction at the single facet lens, relying on a widely used expression (Snyder, 1979) for the photoreceptor angle, which claims that the geometrical acceptance angle and diffraction angle can be convolved as Gaussian functions. It

has been subsequently shown that the Snyder formula is both fundamentally wrong and at variance with experimental data (see van Hateren, 1984; Warrant and McIntyre, 1993; Stavenga, 2004; Stavenga, 2006). Furthermore, as we have concluded above, superposition imaging is not limited by single lens diffraction, which is another reason why the Snyder formula should not be applied. Considering our analysis of the diffraction phenomena in superposition eyes, the conclusion is unavoidable that focusing errors cause the differences between geometrical and experimental acceptance angles.

Angular magnification and defocus

The conclusion that focusing errors are the main cause for a wide acceptance angle leads to the question how the facet lens and crystalline cone modify an incident light beam and what the light distribution in the rhabdom layer is that results from the facet lens–cone optics. Exner (1891) demonstrated already that the facet lens and crystalline cone, which he called a lens cylinder, behave together as an astronomical telescope, and he hypothesized that this was due to gradient refractive indices. Direct measurements on *E. kühniella* (Cleary et al., 1977) and various dung beetles (McIntyre and Caveney, 1985) confirmed Exner's hypothesis. A light ray, entering an astronomical telescope with angle of incidence α, leaves the instrument with an exit angle β, where the angular magnification $m=\beta/\alpha$ equals the ratio of the focal distances of the two lenses that comprise the telescope. Because an astronomical telescope has focal points at infinity, an incident parallel beam leaves the telescope as a parallel exiting beam. This is in slight conflict with the ideal superposition eye concept, which requires that the facet lens and crystalline cone should have a focus at the tip of the rhabdom of the central facet. Therefore, the ideal Exnerian telescope should be modified so that the focal plane coincides with the rhabdom tip. If the light waves leaving the proximal cone tips had spherical phase fronts centered at the rhabdom tip, then diffraction would be the only factor that determines the light distribution in that focal plane.

The calculated Fraunhofer diffraction patterns occur in the focal plane of the imaging optics, that is the facet lens–crystalline cone combination. We had to conclude that in general the focal planes of neighboring facets coincide neither with each other nor with the tip of the rhabdom, and therefore the light distribution pattern resulting from the full superposition aperture will never be a summation of the Fraunhofer diffraction patterns created by the subsequent annuli of coherently collaborating facets. Ray tracing studies (Cleary et al., 1977; McIntyre and Caveney, 1985) did indeed show that the light beams do not have a clear focus or, if there is one, the focus is often quite remote from the rhabdom layer. Although ideally the phase fronts of the light beams leaving the proximal ends of the crystalline cones should have a spherical shape with a distinct center in the rhabdom layer, in reality the phase fronts appear to be rather distorted spheres. Fraunhofer diffraction refers to the focal plane of an optical system, and Fresnel diffraction refers to other planes. The light distribution at the rhabdom entrance will therefore be a summation of Fresnel diffraction patterns broadened by optical errors, which will often be sufficiently large that the potential for creating a crisp superposition image is ruined. Unfortunately, the complex optics of superposition eyes, especially that of the cones, obstructs simple treatments of the imaging process. Careful optical measurements of the optical properties of real eyes will be necessary before further analyses of the imaging details are feasible.

We nevertheless can note that the optical requirements for a reasonably well-focused superposition eye are not extremely severe. The lateral spread of the light beams leaving the crystalline cones and entering the rhabdom layer may be quite restricted, due to the cooperative effect of constructively interfering beams with similar optical path lengths. With a defocus as shown in Fig. 4, a narrow beam still could reach not more than one rhabdom, and thus would not cause a wide acceptance angle.

If defocus indeed does not severely degrade spatial resolution, it would be attractive to make the clear zone width smaller than that requested by ideal superposition. The clear zone is idle space, and it would be logical to economize on that when visual resolution allows it. This may be the reason why the clear zones of both *E. kühniella* and *P. tristifica* are distinctly smaller than that expected from ideal superposition theory (Fig. 4) (see also McIntyre and Caveney, 1998).

The superposition eye of the hawkmoth Macroglossum stellatarum

The hawkmoth *Macroglossum stellatarum*, which is a diurnally active moth, uses an extraordinarily shaped eye (Warrant et al., 1999). Whereas the refractive superposition eyes of moths and skippers studied so far are quite spherical, with negligible gradients in the optics and spatial resolution, the hawkmoth eye is quite aspherical. Measurements of the spatial resolution, using the eye glow, demonstrated that the acuity is extreme anteriorly, with an acceptance angle as low as 1.4°, increasing to twice that value posteriorly. The small acceptance angles were somewhat unexpected, because the deviation from a spherical eye shape was thought to have a deleterious effect on superposition imaging (Warrant et al., 1999). This concern is founded on the assumption that high acuity requires a well-focused superposition eye with a spherical shape, but the case of *P. tristifica* proves that high acuity is possible with a superposition eye that is not well focused. In fact, the data of Warrant et al. show that the superposition aperture spans 13–18 facets (Warrant et al., 1999), and one can estimate that within such a narrow range, the radius of eye curvature will change only slightly, so that the associated change in focus will be within the range of defocus found in other moth eyes that have a constant eye radius and constant angular magnification (Fig. 4). In other words, a spherical shape and perfect focusing at the rhabdom tips is not essential for a superposition eye to realize high quality imaging.

List of symbols

a_i	inner radius of annulus of facets
a_l	lens radius
a_o	outer radius of annulus of facets
B	modified Bessel function
c	joint length of the facet lens and crystalline cone
d	distance between corneal nipples
D_l	lens diameter
D_p	diameter of the ommatidial aperture
D_r	rhabdom diameter
f_l	focal distance of lens
h	nipple height
I	light flux distribution
J	Bessel function
l_c	coherence length
m	angular magnification
n	refractive index
OPL	optical path length
p, p^*	radius of curvature of the proximal cone tips
P, P^*	intersection of α with central ray
q, q^*	distance traveled across clear zone by oblique ray
r, r^*	radius of curvature of the distal surface of the rhabdom layer
R	radius of curvature of the eye surface
s	distance from the axis
T	transmittance
TE	linear polarised light (electric vector perpendicular to the plane of incidence)
TM	linear polarised light (electric vector parallel to the plane of incidence)
u	path length difference of incident rays
w, w^*	width (used for various lengths, see text)
α	angle of incidence
α_{max}	maximal angle of incidence
β	exit angle
β_{max}	maximal exit angle
δ	defocus distance
$\Delta\rho$	acceptance angle of the photoreceptor
$\Delta\lambda$	bandwidth of light
λ	wavelength
θ_l	aperture angle of the facet lens surface
θ_m	angle of incidence at lens margin

This study was inspired by discussions with Dr Roger Hardie and remarks by Dr Andrew Parker. Dr Eric Warrant and two anonymous referees carefully read the manuscript and offered essential, constructive criticisms. The EOARD provided important financial support.

References

Bernhard, C. G. and Miller, W. H. (1962). A corneal nipple pattern in insect compound eyes. *Acta Physiol. Scand.* **56**, 385-386.

Bernhard, C. G., Miller, W. H. and Møller, A. R. (1965). The insect corneal nipple array. *Acta Physiol. Scand.* **63** *Suppl.* **243**, 1-25.

Born, M. and Wolf, E. (1975). *Principles of Optics.* Oxford, New York: Pergamon Press.

Bryceson, K. P. and Mcintyre, P. (1983). Image quality and acceptance angle in a reflecting superposition eye. *J. Comp. Physiol. A* **151**, 367-380.

Cleary, P., Deichsel, G. and Kunze, P. (1977). The superposition image in the eye of *Ephestia kühniella*. *J. Comp. Physiol.* **119**, 73-84.

Exner, S. (1891). *Die Physiologie der facittirten Augen von Krebsen und Insecten.* Leipzig: Deuticke.

Exner, S. (1989). *The Physiology of the Compound Eyes of Insects and Crustaceans* (translated by R. C. Hardie). Berlin, Heidelberg: Springer.

Horridge, G. A., Giddings, C. and Stange, G. (1972). The superposition eye of skipper butterflies. *Proc. R. Soc. Lond. B Biol. Sci.* **182**, 457-495.

Horridge, G. A., McLean, M., Stange, G. and Lillywhite, P. G. (1977). A diurnal moth superposition eye with high resolution *Phalaenoides tristifica* (Agaristidae). *Proc. R. Soc. Lond. B Biol. Sci.* **196**, 233-250.

Kunze, P. (1979). Apposition and superposition eyes. In *Handbook of Sensory Physiology,* Vol. VII/6A (ed. H. Autrum), pp. 442-502. Berlin, Heidelberg, New York: Springer.

Land, M. F. (1981). Optics and vision in invertebrates. In *Handbook of Sensory Physiology,* Vol. VII/6B (ed. H. Autrum), pp. 472-592. Berlin, Heidelberg, New York: Springer.

Land, M. F. (1984). The resolving power of diurnal superposition eyes measured with an ophthalmoscope. *J. Comp. Physiol. A* **154**, 515-533.

Land, M. F. and Nilsson, D.-E. (2002). *Animal Eyes.* Oxford: Oxford University Press.

Land, M. F., Burton, F. A. and Meyer-Rochow, V. B. (1979). The optical geometry of euphausiid eyes. *J. Comp. Physiol. A* **130**, 49-62.

Mandel, L. and Wolf, E. (1995). *Optical Coherence and Quantum Optics.* Cambridge: Cambridge University Press.

McIntyre, P. D. and Caveney, S. (1985). Graded-index optics are matched to optical geometry in the superposition eyes of scarab beetles. *Philos. Trans. R. Soc. Lond. B* **311**, 237-269.

McIntyre, P. D. and Caveney, S. (1998). Superposition optics and the time of flight in onitine dung beetles. *J. Comp. Physiol. A* **183**, 45-60.

Miller, W. H. (1979). Ocular optical filtering. In *Handbook of Sensory Physiology.* Vol. VII/6A (ed. H. Autrum), pp. 69-143. Berlin, Heidelberg, New York: Springer.

Navarro, R. and Franceschini, N. (1998). On image quality of microlens arrays in diurnal superposition eyes. *Pure Appl. Opt.* **7**, L69-L78.

Nilsson, D.-E. (1989). Optics and evolution of the compound eye. *In Facets of Vision* (ed. D. G. Stavenga and R. C. Hardie), pp. 30-73. Berlin, Heidelberg: Springer.

Snyder, A. W. (1979). Physics of vision in compound eyes. In *Handbook of Sensory Physiology*, Vol. VII/6A (ed. H. Autrum), pp. 225-313. Berlin, Heidelberg, New York: Springer.

Stavenga, D. G. (2003). Angular and spectral sensitivity of fly photoreceptors. I. Integrated facet lens and rhabdomere optics. *J. Comp. Physiol. A* **189**, 1-17.

Stavenga, D. G. (2004). Angular and spectral sensitivity of fly photoreceptors. III. Dependence on the pupil mechanism in the blowfly *Calliphora*. *J. Comp. Physiol. A* **190**, 115-129.

Stavenga, D. G. (2006). Invertebrate photoreceptor optics. In *Invertebrate Vision* (ed. E. Warrant and D.-E. Nilsson). Cambridge: Cambridge University Press (in press).

Stavenga, D. G., Foletti, S., Palasantzas, G. and Arikawa, K. (2006). Light on the moth-eye corneal nipple array of butterflies. *Proc. R. Soc. Lond. B* **273**, 661-667.

van Hateren, J. H. (1984). Waveguide theory applied to optically measured angular sensitivities of fly photoreceptors. *J. Comp. Physiol. A* **154**, 761-771.

Vogt, K. (1974). Optische Untersuchungen an der Cornea der Mehlmotte *Ephestia kühniella*. *J. Comp. Physiol.* **88**, 201-216.

Warrant, E. J. and McIntyre, P. D. (1993). Arthropod eye design and the physical limits to spatial resolving power. *Prog. Neurobiol.* **40**, 413-461.

Warrant, E., Bartsch, K. and Günther, C. (1999). Physiological optics in the hummingbird hawkmoth: a compound eye without ommatidia. *J. Exp. Biol.* **202**, 497-511.

Warrant, E. J., Kelber, A. and Kristensen, N. P. (2003). Eyes and vision. In *Handbook of Zoology,*Vol. IV, Pt 36, *Lepidoptera, moths and butterflies*, Vol. 2, *Morphology, physiology and development* (ed. N. P. Kristensen), pp. 325-359. Berlin, New York: Walter de Gruyter.